Study on Flow Field Characteristics and Multi-field Cooperative Mechanism of EGR Valve in Diesel Engine

Yuhang Chen, Cheng Qian*

College of Mechanical and Electrical Engineering, Jiaxing University
* Corresponding author

Abstract: Since EGR valve of diesel engine has a great influence on engine performance, this paper analyzed EGR valve body by CFD numerical simulation method, studied the flow field characteristics of EGR valve in the valve body under different valve lift, and studied the cooperative angle change rule of velocity field and temperature gradient field by applying multi-field coordination theory. The results showed that the exhaust gas passing through EGR reached the maximum air velocity and the lowest temperature after passing through the valve seat. The synergetic Angle varies in a wide range (4.5728°~89.936°) and the synergetic degree is between 7%-8%, indicating that the heat dissipation performance of the whole EGR region is good.

Keywords: EGR; Multi-field collaboration; diesel engine

1. Introduction

Diesel engine has been widely used in automobile industry due to its advantages such as low fuel consumption, high torque output and good reliability [1,2]. However, due to its large emissions, serious environmental pollution, especially particles and NOx, as the main emissions of diesel engines, is the formation of "photochemical smog" the main substances, it must be effectively controlled [3]. Currently, diesel emission control technologies include DPF, SCR and different fuel injection modes [4-6]. However, these methods can no longer meet increasingly stringent emission standards, especially NOx emissions from diesel engines. Currently, the most effective measure to reduce NOx production is the exhaust gas recirculation system (EGR) [7,8]. It is a way of rejoining the combustion by introducing a portion of the exhaust from the engine into the intake manifold. As EGR has a direct impact on engine combustion and emission, the EGR rate used in different working conditions is different. Moreover, the use of EGR will lead to the increase of particulate (PM) and hydrocarbon (HC) emissions in different degrees [9-13], Therefore, the control goal of engine EGR system is to accurately control the EGR rate within a reasonable range [14,15]. The change of EGR rate is mainly guaranteed by the different opening of EGR valve. Therefore, EGR valve is an important component in the exhaust gas recirculation system, and its performance has a direct impact on the NOx emission of the engine [16-18]. Because the high temperature oxygen enrichment is the reason for NOx production, so can be controlled from the oxygen content of the intake, that is, through the exhaust throttle valve and EGR valve as the control input to establish an appropriate EGR rate to change the duty ratio, so as to reduce the maximum explosion pressure, avoid NOx high temperature oxygen enrichment conditions [19-22]. From these research statuses, the opening of EGR valve and the flow through the valve have a decisive influence on engine combustion and exhaust, so the simulation calculation of EGR valve flow channel fluid has research value [23-27]. In this paper, CFD numerical method is used to analyze the flow field characteristics of EGR valve of a certain type of engine under different opening degrees. Meanwhile, the synergistic Angle variation law of velocity field and temperature gradient field is studied by using the field coordination theory, so as to provide a theoretical basis for the subsequent performance improvement of EGR valve.

2. Establishment and Verification of Computational Model

2.1. The Geometric Model

The object of this paper is an EGR valve driven by a stepper motor. Its basic structure is shown in Figure 1. Its EGR rate is controlled by the pulse signal of the stepping motor to push the opening size of the valve body 10. Its flow area can be approximately considered as the inverted cone as shown in Figure 2, and its geometric flow area is calculated as follows:

$$f \approx \pi h'(d_1 + d_2)/2 \approx \pi h \cos\gamma (d_1 + \frac{h}{2}\sin 2\gamma) \quad (1)$$

Where d_1 is the small end diameter of the valve head; γ is the taper Angle of valve seal; h is the valve lift; the meanings of d_2 and h' are shown in Figure 2.

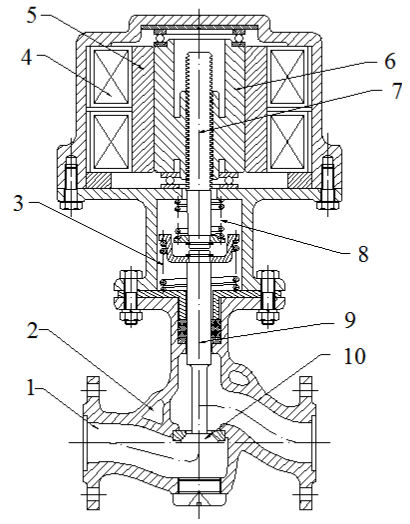

1 exhaust passage; 2 water cooling channels; 3 close the valve spring; 4 the stator coil; 5 the stator pole; 6 the rotor pole; 7 motor shaft; 8 open the valve spring; 9 valve shaft; 10 the valve body

Figure 1. EGR Control valve construction.

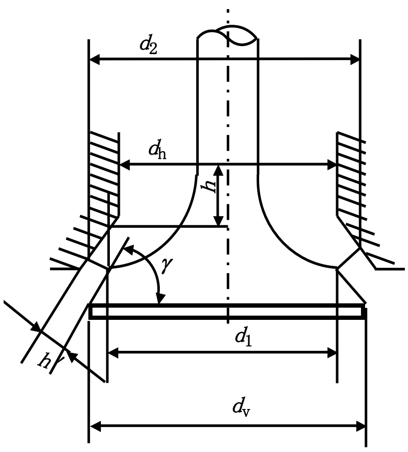

Figure 2. Schematic diagram of valve structure.

The physical parameters of the exhaust gas flowing through EGR valve will change with different working conditions, but the change is small, so it can be ignored. Therefore, the physical parameters of exhaust emissions studied in this paper are shown in Table 1.

Table 1. Physical parameters of engine emissions.

T/K	C_p/(kJ/kg•K)	λ/(W/(m•k))
590	1.0306	0.0411

2.2. The Establishment of Numerical Simulation Model

The flow of high temperature exhaust gas in EGR valve can be regarded as turbulent flow of viscous incompressible fluid and heat exchange between viscous incompressible fluid and wall surface. The flow and heat transfer model include mass conservation equation, momentum conservation equation and energy conservation equation.

Conservation of mass equation:

$$\frac{\partial \rho}{\partial t} + \nabla \cdot \rho \boldsymbol{U} = 0 \tag{2}$$

Where ρ is the density of the fluid, $\boldsymbol{U}$ is the velocity vector of the fluid.

Momentum conservation equation:

$$\frac{\partial(\rho u_i)}{\partial t} + div(\rho u_i \boldsymbol{U}) = -\frac{\partial p}{\partial x_i} + \frac{\partial \tau_{xi}}{\partial x} + \frac{\partial \tau_{yi}}{\partial y} + \frac{\partial \tau_{zi}}{\partial z} + F_i \tag{3}$$

Where p is flow field pressure; $u_i(i=x, y, z)$ is the velocity component of the fluid; τ_{xi} $(i=x, y, z)$ is the component of the viscous stress applied to the microelement body; F_i $(i=x, y, z)$ is the component of the volume force.

Energy conservation equation:

$$\frac{\partial(\rho T)}{\partial t} + div(\rho \boldsymbol{U} T) = div\left(\frac{\lambda}{C_p} gradv\right) - \frac{\partial P}{\partial y} + S_T \tag{4}$$

Where T is absolute temperature; λ is the thermal conductivity of the fluid; C_p is the specific heat capacity of the fluid; S_T is the viscous dissipative term.

Based on the geometric 3d model and flow and heat transfer calculation model, star-CCM+ fluid simulation software was used to analyze the flow field. The computational models were coupling flow model, coupling energy model and RNG k-ε model [28,29]; The entry condition is set as stagnation inlet, inlet pressure value is 120kpa, temperature is 590K, the exit condition is set as pressure outlet, outlet pressure value is 80kpa, temperature is 300K, turbulence is described by setting turbulence intensity and viscosity ratio, and its calculation method is determined by Equations (5) and (6) respectively [30-32]; Set the residual of the corresponding continuity equation as 1×10^{-4}, the residual of the energy equation and the momentum equation as 1×10^{-6} as the iteration termination criterion.

$$I = \frac{\sqrt{u'^2 + v'^2 + w'^2}}{u_{avg}} = 0.16\left(\mathrm{Re}_D\right)^{-\frac{1}{8}} \tag{5}$$

Where u', v', w' is the velocity pulsation quantity, u_{avg} is the average velocity, Re_D is the Reynolds number calculated with hydraulic diameter as characteristic length.

$$\frac{\mu_t}{\mu} = \frac{\rho \cdot C_\mu \cdot k^2}{\varepsilon} \tag{6}$$

Where C_μ is the empirical coefficient, A value of 0.09 is usually assigned; k is the turbulent kinetic energy; ε is the dissipation rate of turbulent kinetic energy.

The numerical simulation model of EGR valve at different valve lifts is shown in Figure 3.

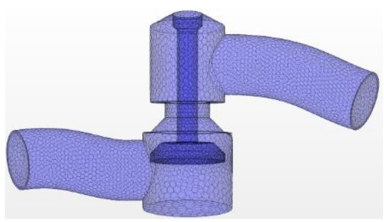

(a) Valve lift is 5mm

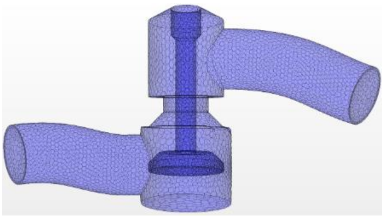

(b) Valve lift is 10mm

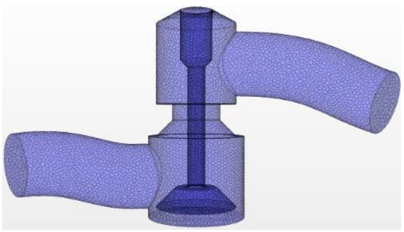

(c) Valve lift is 15mm

Figure 3. Numerical simulation models of different EGR valve lifts.

2.3. Field Synergy Theory

The field synergy principle with enhanced heat transfer technology is taught by Guo Zengyuan [33]. The theory of energy equation analysis for boundary layer type flows has been applied in many fields [34-39]. The theory holds that the heat transfer intensity at the convective heat transfer interface depends not only on the velocity field and the temperature gradient field itself, but also on the Angle between them. The heat transfer process can be regarded as a heat conduction process with an internal heat source, so its energy governing equation can be expressed as a formula (7) [40]:

$$\iiint_{\Omega} \rho C_p \left(\vec{u} \cdot \nabla T\right) dV = \iiint_{\Omega} \nabla\left(\lambda \cdot \nabla T\right) dV \tag{7}$$

Where $\vec{u}$ is the velocity vector; ∇T is temperature gradient; Ω is the calculation domain of fluid heat transfer.

In formula (7), the dot product of the velocity vector and the temperature gradient vector can be expressed by formula (8).

$$\vec{u} \cdot \nabla T = |\vec{u}||\nabla T|\cos(\theta) \tag{8}$$

Where θ is the included Angle between the velocity vector and the temperature gradient vector, namely, the cooperative Angle described in this paper.

Therefore, for the 3-D model of EGR valve, the cooperative Angle of its velocity vector and temperature vector can be expressed as Formula (9).

$$\theta = arc\cos\left(\frac{\frac{\partial T}{\partial x}\cdot u + \frac{\partial T}{\partial y}\cdot v + \frac{\partial T}{\partial z}\cdot w}{\sqrt{\left(\frac{\partial T}{\partial x}\right)^2 + \left(\frac{\partial T}{\partial y}\right)^2 + \left(\frac{\partial T}{\partial z}\right)^2} \cdot \sqrt{u^2 + v^2 + w^2}}\right) \tag{9}$$

Where $\frac{\partial T}{\partial x}$, $\frac{\partial T}{\partial y}$ and $\frac{\partial T}{\partial z}$ is temperature gradients in the *x*, *y* and *z* directions.

In order to study the synergetic degree of convective heat transfer velocity vector field and temperature gradient field, Prof. Guo Zunyuan [41] introduced the concept of synergy coefficient, namely, the ratio of the cosine of the synergy Angle greater than 0.8 to the total flow field area λ_{FSP} as shown in Equation (10):

$$\lambda_{FSP} = \frac{\sum_{\cos\theta_i \geq 0.8}^{\cos\theta_i \leq 1} \cos\theta_i}{\sum_{\cos\theta_i \geq 0}^{\cos\theta_i \leq 1} \cos\theta_i} \times 100\% \tag{10}$$

3. The Simulation Analysis

3.1. Flow Field Simulation Analysis of EGR Valve

The fluid flow simulation of EGR valve with lift of 5mm, 10mm and 15mm established above obtained the corresponding velocity vector field and temperature field. The symmetrical center surface of EGR valve was taken as the auxiliary plane, and the velocity vector field and temperature field were respectively shown in Figure 4 and Figure 5.

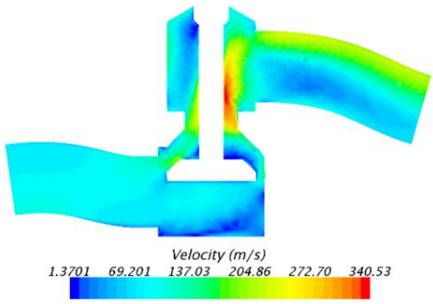

(a) Valve lift is 5mm

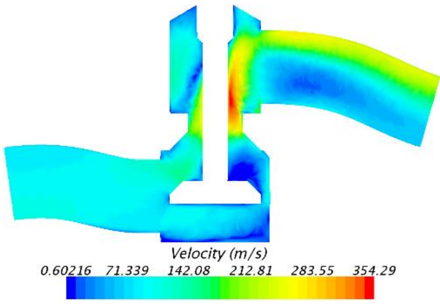

(b) Valve lift is 10mm

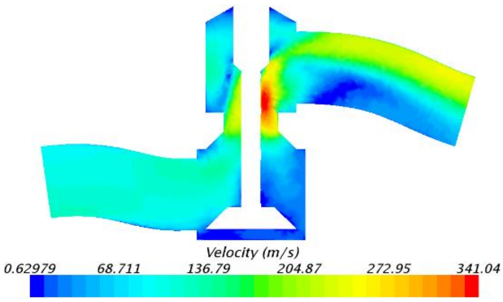

(c) Valve lift is 15mm

Figure 4. Velocity vector field of different EGR valves in lift.

As can be seen from the velocity vector field in Figure 4 under different valve lifts, the exhaust gas passing through EGR after passing through the valve seat can reach more than 340m/s due to the narrow gap between the seat and the wall surface, and the velocity of flow field in different areas varies greatly.

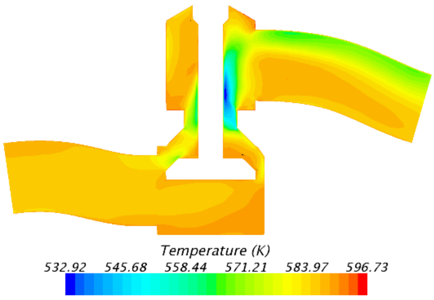

(a) Valve lift is 5mm

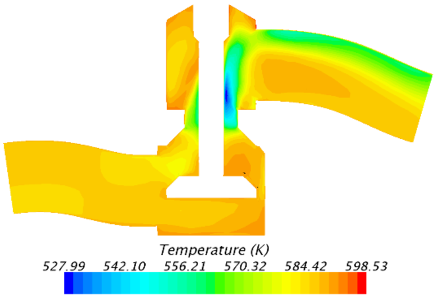

(b) Valve lift is 10mm

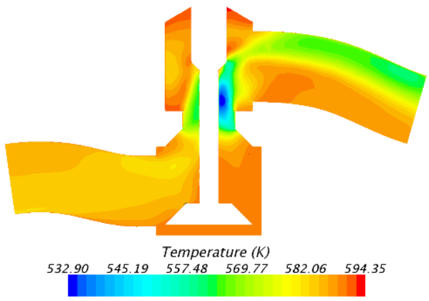

(c) Valve lift is 15mm

Figure 5. Temperature field of EGR at different valve lifts.

As can be seen from Figure 5, the temperature difference in the whole flow field area is around 60K, and the lowest temperature area appears behind the valve seat, which is due to the large gas velocity in this area and the loss of part of internal energy, which leads to a decrease in temperature.

3.2. Co-simulation Analysis of EGR Valve Field

By applying the conclusion of flow field analysis and equations (9) and (10) of field coordination theory, the velocity vector field and temperature gradient field in the flow field of EGR valve were simulated and analyzed, and the coordination Angle distribution diagram of symmetrical center surface in the flow field was obtained as shown in Figure 6.

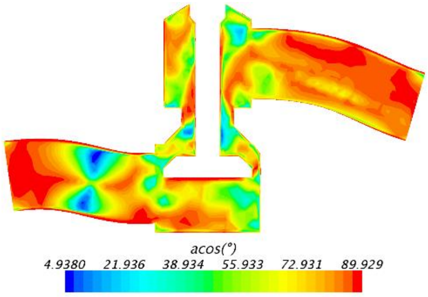

(a) Valve lift is 5mm

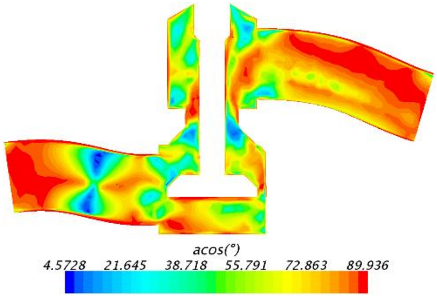

(b) Valve lift is 10mm

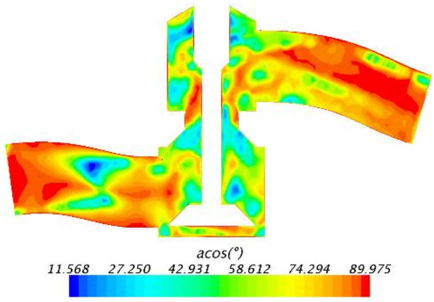

(c) Valve lift is 15mm

Figure 6. Coordination Angle under different EGR valve lifts.

From figure 6 of synergy Angle under different valve lift, you can see that the engine EGR valve internal field synergy Angle change is bigger, in point of smaller area of the flow field, the disturbance is larger, especially around the valve inlet and body, it shows that the cooling performance is good, these regions is beneficial to reduce the exhaust gas temperature can be rapidly after, thereby improving the performance of the EGR valve. The synergetic degree of the entire flow field region is analyzed according to Equation (10), and the results are shown in Table 2.

Table 2. Results of the field synergy calculation.

Valve lift /mm	Synergy degree λ_{FSP}
5	8.84%
10	7.81%
15	7.23%

The statistical results in Table 2 show that the field coordination degree of the whole flow field region is between 7%-8%, maintaining a good heat transfer performance.

4. Conclusions

In this paper, the flow field characteristics and multi-field cooperative mechanism of EGR valve driven by stepping motor are analyzed, and numerical simulation models of EGR valve under different valve lifts are established to obtain the flow field characteristics and multi-field cooperative characteristics under different valve lifts.

(1) Results can be obtained by the velocity field and temperature field: after an EGR after the exhaust valve seat, due to the seat and the wall of the narrow gap, maximum flow rate, at the same time, because of the large gas flow velocity in the region lost a part of that can lead to a drop in temperature, showing the area for the entire flow field area of minimum temperature zone.

(2) The multi-field coordination results based on temperature gradient and velocity field show that the coordination Angle varies widely (4.5728°~89.936°) in the whole flow field region, and the coordination degree is between 7%-8%, indicating that the heat dissipation performance of the whole EGR region is better.

References

[1] Maghbouli, A.; Yang, W.M.; An, H.; Li, J.; Chou, S.K.; Chua, K.J. An advanced combustion model coupled with detailed chemical reaction mechanism for D.I diesel engine simulation. *Appl. Energy* **2013**, 111, 758–770.

[2] Maghbouli, A.; Yang, W.M.; An, H.; Shafee, S.; Li, J.; Mohammadi, S. Modeling knocking combustion in hydrogen assisted compression ignition diesel engines. *Energy* **2014**, 76, 768–779.

[3] Brijesh, P.; Chowdhury, A.; Sreedhara, S. Effect of Ultra-Cooled EGR and Retarded Injection Timing on Low Temperature Combustion in CI Engines. SAE 2013 World Congress & Exhibition, Detroit: SAE International, 2013-01-0321

[4] Benajes, J.; Molina, S.; García, A.; Monsalve-Serrano, J. Effects of low reactivity fuel characteristics and blending ratio on low load RCCI (reactivity controlled compression ignition) performance and emissions in a heavy-duty diesel engine. *Energy* **2015**, 90, 1261–1271.

[5] Paykani, A.; Kakaee, A.H.; Rahnama, P.; Reitz, R.D. Effects of diesel injection strategy on natural gas/diesel reactivity controlled compression ignition combustion. *Energy* **2015**, 90, 814–826.

[6] Zhou, D.Z.; Yang, W.M.; An, H.; Li, J. Application of CFD-chemical kinetics approach in detecting RCCI engine knocking fuelled with biodiesel/methanol. *Appl. Energy* **2015**, 145, 255–264.

[7] Xie, F.X.; Hong, W.; Su, Y.; et al. Effect of external hot EGR dilution on combustion, performance and particulate emissions of a GDI engine. *Energy Conversion and Management* **2017**, 142, 69-81.

[8] Yanuandri P.; Narankhuu J.; Ocktaeck L. An investigation on the DME HCCI autoignition under EGR and boosted operation. *Fuel* **2017**, 200, 447-457.

[9] Zhang, Q.; Li, M.H.; Li, G.X.; et al. Transient emission characteristics of a heavy-duty natural gas engine at stoichiometric operation with EGR and TWC. *Energy* **2017**, 132, 225-237.

[10] Pedrozo, V.B.; May, I.; Zhao, H. Exploring the mid-load potential of ethanol-diesel dual-fuel combustion with and without EGR. *Applied Energy* **2017**, 193, 263-275.

[11] Lattimore, T.; Wang, C.M.; Xu, H.M.; et al. Investigation of EGR Effect on Combustion and PM Emissions in a DISI Engine. *Applied Energy* **2016**, 161, 256-267.

[12] Zhang, Q.; Xu, Z.S.; Li, M.H.; Shao, S.D. Combustion and emissions of a Euro VI heavy-duty natural gas engine using EGR and TWC. *Journal of Natural Gas Science and Engineering* **2016**, 28, 660-671.

[13] Rajesh kumar, B.; Saravanan, S. Effect of exhaust gas recirculation (EGR) on performance and emissions of a constant speed DI diesel engine fueled with pentanol/diesel blends. *Fuel* **2015**, 160, 217-226.

[14] Midhat, T.; Paul, H.; Nicos, L. The effect of varying EGR and intake air boost on hydrogen-diesel co-combustion in CI engines. *International Journal of Hydrogen Energy* **2017**, 42(9), 6369-6383.

[15] Cho, J.; Song, H.H. Understanding the effect of external-EGR on anti-knock characteristics of various ethanol reference fuel with RON 100 by using rapid compression machine. *Proceedings of the Combustion Institute* **2017**, 36(3), 3507-3514.

[16] Huang, H.Z.; Liu, Q.S.; Wang, Q.X.; et al. Experimental investigation of particle emissions under different EGR ratios on a diesel engine fueled by blends of diesel/gasoline/n-butanol. *Energy Conversion and Management* **2016**, 121, 212-223.

[17] Mina, N.; Masato, K.; Norimasa, I. Assessment for innovative combustion on HCCI engine by controlling EGR ratio and engine speed. *Applied Thermal Engineering* **2016**, 99, 42-60.

[18] José, M.L.; Héctor, C.; Ricardo, N.; Manuel, E.R. Influence of a low pressure EGR loop on a gasoline turbocharged direct injection engine. *Applied Thermal Engineering* **2015**, 89, 432-443.

[19] Ádám, B.; Huba, N. Model development for intake gas composition controller design for commercial vehicle diesel engines with HP-EGR and exhaust throttling. *Mechatronics* **2017**, 44, 6-13.

[20] Subir, B.; Hervé, J.; Francesco, C. Tar Tolerant HCCI Engine Fuelled with Biomass Syngas: Combustion Control Through EGR. *Energy Procedia* **2017**, 105, 1764-1770.

[21] Divekar, P.S.; Chen, X.; Tjong, J.; et al. Energy efficiency impact of EGR on organizing clean combustion in diesel engines. *Energy Conversion and Management* **2016**, 112, 369-381.

[22] Xie, F.X.; Li, X.P.; Su, Y.; et al. Influence of air and EGR dilutions on improving performance of a high compression ratio spark-ignition engine fueled with methanol at light load. *Applied Thermal Engineering* **2016**, 94, 559-567.

[23] Samad, J.; Peyman, N.; Rana, K. Multidimensional modeling of the effect of Exhaust Gas Recirculation (EGR) on exergy terms in an HCCI engine fueled with a mixture of natural gas and diesel. *Energy Conversion and Management* **2015**, 105, 498-508.

[24] Mohsen, M.K.; Shahram, K.; Arash, N. A numerical investigation on the influence of EGR in a supercharged SI engine fueled with gasoline and alternative fuels. *Energy Conversion and Management* **2014**, 83, 260-269.

[25] Samad, J. Multidimensional modeling of the effect of EGR (exhaust gas recirculation) mass fraction on exergy terms in an indirect injection diesel engine. *Energy* **2014**, 66, 305-313.

[26] Pan, M.Z.; Shu, G.Q.; Wei, H.Q.; et al. Effects of EGR, compression ratio and boost pressure on cyclic variation of PFI gasoline engine at WOT operation. *Applied Thermal Engineering* **2014**, 64, 491-498.

[27] Cung, K.; Moiz, A.A.; Zhu, X.C.; Lee, S.Y. Ignition and formaldehyde formation in dimethyl ether (DME) reacting spray under various EGR levels. *Proceedings of the Combustion Institute* **2017**, 36(3), 3605-3612.

[28] Manimaran, R.; Thundil Karuppa Raj, R. CFD Analysis of Combustion and Pollutant Formation Phenomena in a Direct Injection Diesel Engine at Different EGR Conditions. *Procedia Engineering* **2013**, 64, 497-506.
[29] Kosmadakis, G.M.; Rakopoulos, C.D.; Demuynck, J.; et al. CFD modeling and experimental study of combustion and nitric oxide emissions in hydrogen-fueled spark-ignition engine operating in a very wide range of EGR rates. *International Journal of Hydrogen Energy* **2012**, 37(14), 10917-10934.
[30] Bayazid, M.; Seyyed, H. H.H.; Goodarz, A.; et al. CFD simulation of reactor furnace of sulfur recovery units by considering kinetics of acid gas (H2S and CO2) destruction. *Applied Thermal Engineering* **2017**, 123, 699-710.
[31] Christian, B.; Yang, J.F.; Larsson, H.; et al. Evaluation of mixing and mass transfer in a stirred pilot scale bioreactor utilizing CFD. *Chemical Engineering Science* **2017**, 171, 19-26.
[32] Koh, W.X.M.; Ng. E.Y.K. A CFD study on the performance of a tidal turbine under various flow and blockage conditions. *Renewable Energy* **2017**, 107, 124-137.
[33] Guo, Z.Y.; Tao, W.Q.; Shah, R.K. The field synergy (coordination) principle and its applications in enhancing single phase convective heat transfer. *Int J Heat Mass Transf*, **2005**, 48, 1797-807.
[34] Yang, J.; Ma, L.; Liu, J.J.; Liu, W. Thermal–hydraulic performance of a novel shell-and-tube oil cooler with multi-fields synergy analysis. *Int J Heat Mass Transf* **2014**, 77, 928-939.
[35] An, L.S.; Yang, Z,; Zhong, G.Y.; Liu, Y.W. Improvement of Heat and Mass Transfer Performance in a Polysilicon Chemical Vapor Deposition Reactor with Field Synergy Principle. *Energy Procedia*, **2017**, 105, 688-693.
[36] Li, X.; He, Y.L.; Tao, W.Q. Analysis and extension of field synergy principle (FSP) for compressible boundary-layer heat transfer. *International Journal of Heat and Mass Transfer*, **2015**, 84, 1061-1069.
[37] Mohammed, O.A. Hamid, B.Z. Field synergy analysis for turbulent heat transfer on ribs roughened solar air heater. *Renewable Energy*, **2015**, 83, 1007-1019.
[38] Jiaqiang, E.; Zhao, X.H.; Liu, H.L.; et al. Field synergy analysis for enhancing heat transfer capability of a novel narrow-tube closed oscillating heat pipe. *Applied Energy*, **2016**, 175, 218-228.
[39] Xia, G.D.; Li, Y.F.; Wang, J.; Zhai, Y.L. Numerical and experimental analyses of planar micromixer with gaps and baffles based on field synergy principle. *International Communications in Heat and Mass Transfer* **2016**, 71, 188-196.
[40] Tao, W.Q.; Guo, Z.Y.; Wang, B.X. Field synergy principle for enhancing convective heat transfer-Its extension and numerical verifications, *Int J Heat Mass Transf* **2002**, 45, 3849-3856.
[41] Guo, Z.Y.; Li, D.Y.; Wang, B.X. A novel concept for convective heat transfer enhancement. *Int J Heat Mass Transf*, **1998**, 41, 2221–2225.